I.T.C

Content list available at ITC

Techno-Science Research Journal

Journal Homepage: www.itc.edu.kh

Techno-Science Research Journal

Responses of Diluted Slurry-Filled Tube Subjected to Axial Impact Loading

K. Nguon[1*], K. Inaba[2], H. Takahashi[2], K. Kishimoto[2]

[1]Department of Industrial and Mechanical EngineeringInstitute of Technology of Cambodia, CAMBODIA
[2]Department of Mechanical Sciences and Engineering, Tokyo Institute of Technology, JAPAN

Abstract: *Strongly coupled fluid-structure interaction (FSI) between diluted slurry of water and $CaCO_3$ particles and a polycarbonate tube was studied numerically. A steel piston was impacted on top of the slurry, causing the generation and propagation of flexural waves in the tube wall and pressure waves in the slurry. Considering homogeneous mixtures as slurry and using the Arbitrary Lagrangian-Eulerian method, FSI cases with different volume fractions of solid particles were considered. It was revealed that the wave speeds in the slurry were lower than those in water and tended to decrease gradually with an increase in the volume fraction of the particles. On the other hand, the pressures were less dependent on the volume fraction of particles in the slurry. Numerical results agreed well with the theoretical results proposed by Han et al. (1998), and the main trend of our experimental findings was shown.*

Keywords: Impact tube response, fluid-structure interaction, water hammer, diluted slurry

1. INTRODUCTION

Solid-liquid coupling plays very important role in transient dynamics, which has been available in a number of publications. The majority of the reviewed documents highlighted the characteristic of "*water hammer*" that is also referred to *pressure surges* or *transient flows*(Tijsseling, 1993). Analyses of the FSI in the diluted slurry are conducted with a single liquid and the mixtures of water and fine particles producing low concentration usually referred to homogeneous mixture.

In engineering practice, fluid-structure interaction (FSI) in pipes has caused a number of serious damages. Two failures have occurred in nuclear power plants because of detonation loading inside the pipe system: Hamaoka-1 NPP in Japan and Brunsbüttel KBB in Germany (Shepherd, 2009). In these accidents, detonable mixtures were accumulated by radiolysis and water was present near the explosion site. It is quite likely that the impact-loaded water interacted with the tube wall, caused FSI, and increased the damages during the explosions. In common industrial applications, a liquid-filled pipe may experience such an event, for example, by the fast closure of check valves. As a compression wave in the liquid propagates perpendicular to the submerged structure, flexural waves are also generated. The main wave propagation mode is flexural, and it is closely coupled to a pressure wave in the liquid. Dynamic forces generated in a water hammer event can make the system move and generate significant FSI. As a result, the liquid and pipe systems cannot be treated separately in a theoretical analysis. In the majority of the studies carried out thus far, the propagation of transients in axisymmetric elastic and viscoelastic fluid-filled pipes has been analyzed using various 1-D theories. Techniques for determining the relevant mechanical parameters of system components have been developed for slender, straight,

[*]Coresponding authors:
E-mail: seangmeng@itc.edu.kh; Tel: +855-78-406-183; Fax: +855-23-880-369

prismatic and thin-walled circular cross-section pipes. According to Barez et al., (1979), a streaming fluid rather than a stationary one has no effects on the wave speeds when the ratio of flow velocity to wave propagation speed is greater than 10^{-3}. However, it has been reported experimentally that the wave speeds in slurry-filled pipes are slightly greater than those in empty pipes, owing to FSI. Skalak (Skalak, 1955/1956; Skalak, 1956) extended the theory of water hammer event to axisymmetric thin-walled pipes. In his mathematical models, the effects of radial inertia of liquid and pipe and the longitudinal stress waves in the wall were considered to describe deflection-free wave propagation in liquid-filled pipes. Moreover, Tijsseling et al., (2008) tried to extend Skalak's theory by assessing the dispersion of pressure waves and concluded that in unrestrained water-filled steel and plastic pipes, wave-front spreading owing to FSI is small, at the most of the order of 10 pipe diameters. Han et al., (1998) derived the equations for slurry hammer to estimate the wave propagationspeeds and pressure variations in pseudo-homogeneous. His results agreed well with the estimations of wave speeds and pressure jump for iron and phosphorus slurries. However, the theoretical and experimental wave speeds for coal suspensions showed a discrepancy.

2. BASIC EQUATIONS

In the classical theories, FSI problems in the case ofslurry had been predicted to be different fromthe case of water only due to the change in fluid properties such as density and bulk modulus. In the slurry form, the density of the mixture, ρ_m,can be calculated in function of the volume fraction of the solid particles, C_v, and the fluid and solid density, ρ_f andρ_s , respectively.

$$\rho_m = \rho_s C_v + (1 - C_v)\rho_f. \quad (1)$$

The Rule of Mixtures gives the bulk modulus of slurry in form of

$$K_m = 1/[(C_v/K_s) + (1 - C_v)/K_f] \ldots \quad (2)$$

The unconfined sound speed of the fluid, C_f, depends on the bulk modulus and its density given by

$$C_f = \left(\frac{K_f}{\rho_f}\right)^{1/2}. \quad (3)$$

In a solid rod of Young modulus $E_s$and density ρ_s, its sound speed can be calculated with

$$C_s = \left(\frac{E_s}{\rho_s}\right)^{1/2}. \quad (4)$$

The water hammer wave speeds can be estimated by the Korteweg-Joukowsky speed [2.3, 2.4].

$$C = \left(\frac{C_f}{1+\frac{2rK}{tE_p}}\right)^{1/2}. \quad (5)$$

taking into account the Young's modulus E_p of the pipe having the medium diameter r and wall-thickness t. The Korteweg-Joukowsky speed equation predicts the decrease of the wave speed as the bulk modulus of fluid increases.

The water hammer wave speed is used to predict the pressure jump Δp proposed by Joukowsky (Joukowsky, 1900):

$$\Delta p = \rho C \Delta u. \quad (6)$$

whereΔu is the change in the velocity of the flow. The Joukowsky equation estimates the increase of the pressure jump with the increasing volume fraction.

3. NUMERICAL MODELS

We modeled tubes with a length of 180 mm, inner diameter of 52 mm, and wall thickness of 4 mm (Fig. 1). These models were obtained by downsizing our previous experimental setup (Souli et al., 2000); we tested a 1-m tube of the same cross-section, wall thickness, and material by using a projectile impact. Very fine $CaCO_3$ powders (averaged diameter of 6 □m) of different volume fractions (the maximum volume fraction is 12.5%) were mixed to form slurries. A plastic buffer mounted within the tube was stroked by a piston accelerated by gravity at a speed of 0.7 m/s to generate waves within the slurry and tube specimen.In the present model, the tube and fluid bottom were fixed with a rigid plate to ensure that the tube and fluid subjected to impact load were prevented from moving forward so that the active parts in contact with the rigid plate did not have any degrees of freedom. The steel piston was impacted downward on the surface of the stationary fluid (at a distance of 150 mm from the fixed bottom end of the tube) with an initial velocity of 1 m/s. The friction between active parts of piston–tube, piston–fluid, and fluid–tube was neglected. The details of the geometry and material properties of the models are shown in Fig. 1 and Table 1.

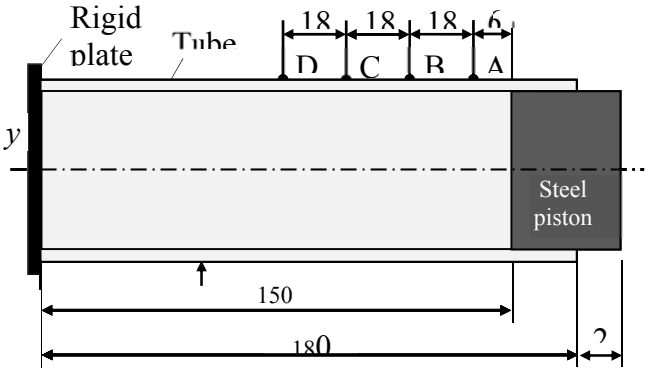

Fig.1. Experimental peak strains (g8) normalized by incident peak strain (g1) around particles.

The governing equations of mass, momentum, and energy conservation are given for the fluid and the tube, which follow the Arbitrary Lagrangian-Eulerian(ALE) method (Souli et al., 2000; Aquelet et al., 2005). The pressure outside the tube was not modeled. For simplicity, water and slurry were assumed to be inviscid fluid. We also assumed that the slurry is the homogeneous mixture where there are no actual solid particles but density and bulk modulus change with the volume fraction of the particles.

Table 1 Geometrical and material properties of models

Properties	Polycarbo- nate tube	Steel piston	$CaCO_3$ particles	Water column
Outer radius [mm]	*30*	26	-	26
Length [mm]	*180*	50	-	150
Wall thickness [mm]	*4*	-	-	-
Mass density [kg/m^3]	1220	7850	2710	1000
Poisson's ratio	0.37	0.30	-	-
Young's modulus [GPa]	2.45	210	70.0	-
Bulk modulus [GPa]	-	-	23.3	2.2

Either in the form of water or slurry, the fluid was modeled as a null material for which the shear stiffness and yield strength are neglected. Such a kind of fluid requires an equation of state expressed by the Grüneisen equation (Livemore, 2007) that defines pressure as

$$p = \frac{\rho_f C_f^2 \mu \left[1 + \left(1 - \frac{\gamma_0}{2}\right)\mu - \frac{a}{2}\mu^2\right]}{\left[1 - (S_1 - 1)\mu - S_2 \frac{\mu^2}{\mu+1} - S_3 \frac{\mu^3}{(\mu+1)^2}\right]^2} + (\gamma_0 + a\mu)E \qquad (7)$$

where C_f is the unconfined sound speed of water or slurry; a is the first order volume correction to Grüneisen gamma γ_0; ρ_0 and ρ_f are the reference and current density, respectively; E is the absolute internal energy and $\mu = (\rho/\rho_f) - 1$; and S_1, S_2, and S_3 are the coefficients of the slope of the shock velocity-particle velocity curve (Meyers, 1994).

Table 2 Fluid properties and water hammer characteristics with classical theories

Parameters	Water	4% slurry	8% slurry	12% slurry
Density ρ_f [kg/m^3]	*1000*	1068	1137	1205
Bulk modulus K_f [GPa]	*2.200*	2.282	2.371	2.468
Unconfined sound speeds C_f [m/s]	*1483*	1461	1444	1431
Korteweg wave speed C [m/s]	412.7	399.8	388.2	377.5
Pressure jump Δp [kPa]	413	427	441	455

4. RESULTS AND DISCUSSION

When kinematic energy was generated by the piston, the pressure inside the tube increased, which caused compression and stress wave propagation in the tube. Deformed model modes in Fig. 2 were exaggerated to capture the modes of fluid and structural deformations. The waves propagating along loading direction are divided into 2 types; the precursor wave (light dark color directed by a gray arrow) that has small amplitude and travels at a speed close to the sound speed in the tube and the primary wave or flexural wave (dark color directed by a dark arrow) that is the main disturbance causing significant change of the cross-section of the fluid and tube. Therefore, the latter was taken into account in the present investigation. The primary wave usually travels at a lower speed than the sound speed in the unconfined fluid.

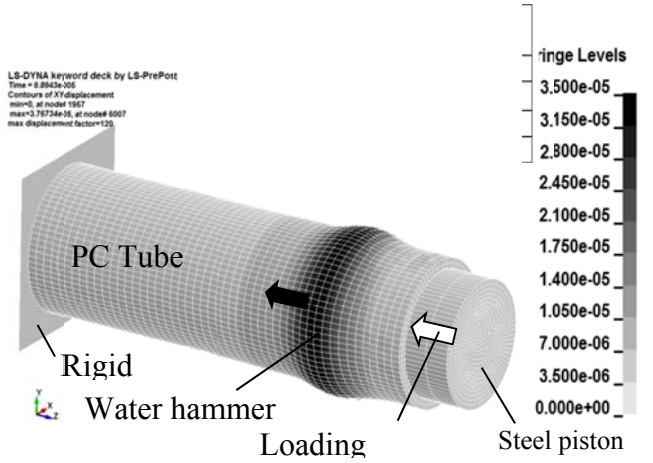

Fig.2.Tube model in case of water at t = 0.069 ms (Displacement scale factor: X = 100, Y = 100, and Z = 1)

a. Water-pipe coupling

The filled-fluid was characterized as a water column with the same inner cross-section of the tube and length of 150 mm. In this model, we observed the displacement at

some locations (from A to D) selected incrementally at 18 mm along the outer tube surface (See Fig. 1). Location A is near the top of the tube at 6 mm from the bottom of the piston and 54 mm from location D. We also measured the peak pressure at selected elements along the surface of the fluid model, just beneath the selected points on the tube. The changes in the cross-section of the fluid were observed at these locations because they do not depend on the effect of the reflection of the precursor wave. Hoop strains were obtained from the displacements of the tube specimen captured in the *XY*-direction by simply calculating the ratio between the radius displacement to the pipe outer radius,$\Delta r/r$. At the initiating process, the distance between the precursor wave and primary wave was too close to be captured separately.

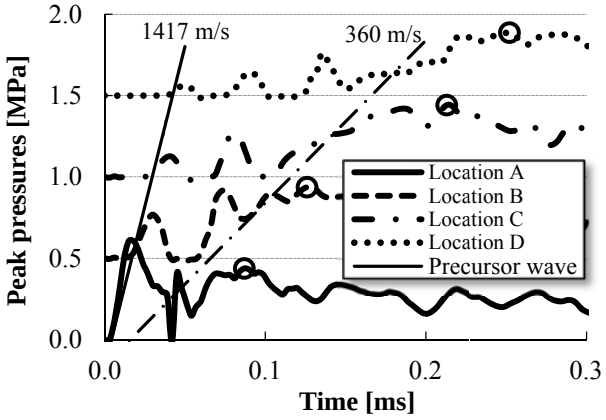

Fig.3. Pressures of water columns

The strain of 0.75 m corresponding to a distance of 18 mm on the fluid model was shifted incrementally to compare the change in strain at different locations. The 0.4-m threshold of hoop strain of was selected to determine the arrival time of the primary wave front. The primary water hammer wave propagated at a speed of around 360 m/s (dashed baseline) whereas the unconfined sound propagated at a speed of 1483 m/s. The unconfined sound speed of water was slightly higher than that of the precursor wave known to be close to the sound speed of the polycarbonate tube, 1417 m/s (continuous baseline). The model gave small changes in hoop strains measured at several nodes, which implied that stress waves propagated at almost constant velocity along and within the pipe. The maximum hoop strains were marked with small blank circles on the curves giving the averaged maximum hoop strain of 1.13 m.

The fluid column kinematic energy from the piston results in compression and wave propagation along the tube and fluid. The continuous baseline in Fig. 3 presents the precursor wave and another baseline indicates the primary wave passing through the selected elements. The first peak of each pressure curve occurred with the influence of the precursor wave, whereas the peak pressure marked by the blank circle represents the peak pressure corresponding to the primary wave, 360 m/s (dashed baseline). The averaged peak pressure of 426 kPa obtained in this model is comparable with the theoretical peak pressure of 413kPa(Table 3). A dramatic decrease in pressure was captured in the time interval of between 0.03 and 0.06 msbehind the precursor wave front. This occurrence might be provoked by the radial oscillation in the fluid due to tube expansion as shown in Fig. 2.

b. Slurry hammer

Very fine calcium carbonate particles ($CaCO_3$) of 2710 kg/m^3 mass density, bulk modulus of 23.3 GPa, and Young's modulus of 70.0 GPa were modeled as mixtures with water for obtaining slurries of different volume fractions (C_v). Different from the experimental work, the vacuum condition of the specimen was obtained in the numerical models, which enabled us to neglect the effect of air in the results.

In the case where the tube was filled with slurry of 4% C_v, the water hammer wave speed decreased to 353 m/s with the decrease of the unconfined sound speed in the slurry to 1461 m/s (Tables 2 and 3). This tendency may be influenced by the effect of density rather than the bulk modulus, and such an effect can be described by the Eq. (3). In addition, the averaged peak pressure of 436 kPa showed a slight increase if compared with that in the case of water.

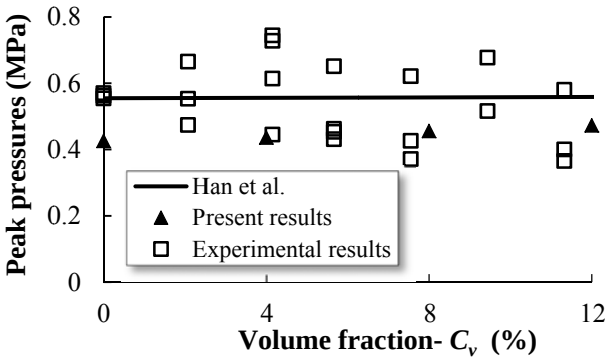

Fig.4. Pressures of water columns

The overall observation in the case of slurry was performed similarly to the previous case. Figure 6 indicates that the change in the volume fraction of $CaCO_3$ particles has little influence on the pressures. This trend is in the good agreement with all three analysis methods: theory, simulation, and experiment. Experimental pressures represented by blank squares were obtained using a piezoelectric transducer mounted at the bottom of the tube specimen where an aluminum plug was used and treated as a rigid plate to obstruct the forward motion of the tube and

the fluid undergoing the impact load of the piston (Souli et al., 2000).

The experimental results in Fig. 4 represent the reflected pressures which are almost twice (×1.94) as large as the pressure jump defined by Eq. (6) due to the primary wave. Because Han's theory did not include this effect, Han's theoretical pressure in Fig. 4 was drawn by multiplying with 1.94. This factor was obtained by the impedance mismatching method using the acoustic impedances of Al and water [13]. Theoretical pressures (Jokowsky, 1900) slightly increase from 0.55 MPa to 0.56 MPa with increasing C_v from 0% to 12%. The fluid pressures (filled triangles) obtained from the numerical simulations did not differ much from one case to another (different C_v), in the range of 2%–4%, (Table 3). Although the numerical simulations indicated lower pressure peaks compared with the experimental and theoretical results, the numerical results are actual peak pressures due to the primary wave and are not doubled by the reflection effect. Moreover, the piston speed in the numerical simulations is 1.0 m/s and faster than the 0.7 m/s speeds in the experiments. If we consider the reflection and difference of the piston speed (v_0= 0.7 m/s), the numerical reflected pressure (for example, the case of water) is evaluated as 0.57 MPa (=0.426×1.94×0.7) and agrees well with the experimental and theoretical pressures.

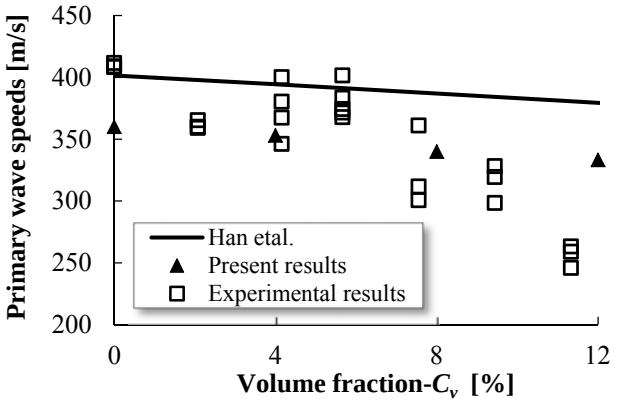

Fig. 5 Relationship between primary wave speeds and volume fraction of particles.

Moreover, it is found that the primary wave propagating along the wall tends to decrease gradually with lowering sound speed of the fluid in the slurry as the particle volume fraction is increased. It can be seen in Fig. 5 that the present numerical wave propagation speeds agree well with the results obtained from experiments using impact speeds of 0.7 m/s (Inaba et al., 2010) and theoretical estimations. This trend compares well with the models and theoretical work (Conceicao et al., 2003) as the volume fraction increases. In the three analysis methods, the wave speed is less dependent on the impact speed. A change in the volume fraction causes significant decrease of the experimental primary wave speeds. This discrepancy may be influenced by viscosity effects in the mixture. Shear response of $CaCO_3$ suspensions indicated that relative viscosity with C_v = 12.5% is 1.6 times higher than those of water (Kugge et al., 2004). In general, the slurries with $C_v \leq$ 10% are characterized as Newtonian fluid (Russel et al., 1989). However, the stress-strain curve of $CaCO_3$ suspensions for $C_v \geq$ 20% exhibits pseudoplastic-type (non-Newtonian) behavior with shear stress (Conceicao et al., 2003). In the future work, we will examine the effect of viscosity including the contact friction and the applicability of the governing equations (Navier-Stokes equations). The other possibility of the discrepancy may be the interaction between particles and the wave-front due to non-homogeneity in the mixture or the presence of air; a small percentage of air causes a large reduction in the wave speed.

The results of the measured pressure and wave propagation speeds are also listed in Table 3. Inspection of Fig. 5 reveals that the maximum hoop strains measured at selected locations are slightly different. Subsequently, they were averaged in the case of water and slurry, which indicated a little increase with increasing volume fraction of particles. These results are comparable with the hoop strains estimated with Tijsseling's equation (Tijsseling, 2007) when the averaged internal pressures were substituted into his thick-wall equation.

$$\varepsilon_{hT} = \frac{1}{E_{tube}}\left[\frac{r}{t}\frac{\left(p_{in}-p_{out}\right)}{1+\dfrac{t}{2r}} - \left(1-\nu_{tube}\right)p_{out}\right] \qquad (8)$$

where r is the mean of the inner and outer radii (28 mm in the present models) and t represents the tube wall-thickness (4 mm).

The primary wave speeds obtained from the models show a decreasing trend with a slight change with each case fluid, which agrees well with the wave speeds estimated with Eq. (8) as indicated in Tables 2 and 3.

Table 3 Summary of results

Parameters	Water	4% Slurry	8% Slurry	12% Slurry
Primary wave speed* C_w [m/s]	*360*	353	340	333
Peak pressure* P_{ave} [kPa]	*426*	436	456	473
Maximum hoop strain* ε_{hN}[mε]	*1.13*	1.15	1.18	1.21
Theoretical hoop strain** ε_{hT} [mε]	*1.14*	1.16	1.22	1.26

(*) Numerical results
(**) Theoretical predictions proposed by Tijsseling (Tijsseling, 2007).

5. CONCLUSIONS

Strongly coupled fluid-structure interaction between slurry and a polycarbonate tube has been investigated numerically by using the finite element code LS-DYNA_971. Numerical wave speeds along the water-filled tube are in good agreement with the current experimental data and theoretical estimations proposed by Han *et al*. However, there are discrepancies between the results obtained using the models and the experimental results in the case of slurry with a high volume fraction of particles. In addition, the computational results are validated as the hoop strains in all models reveal excellent agreement with Tijsseling's thick-wall equation.

Numerical results indicate that the increasing percentage of particles in the slurry decreases the primary wave propagation speeds but restrains the pressures, as the reported theoretical and experimental findings consistently show less dependence on pressure. The main trend has been shown between the present results and theoretical findings. Non-homogeneity and viscosity effects on the slurry will be included in future investigations.

REFERNCES

Aquelet, N., Seddon, C., Souli, M. and Moatamedi, M.,, (2005).Initialisation of Volume Fraction in Fluid/Structure Interaction Problem, *International Journal of Crashworthiness*, Vol.10.

Barez, F., Goldsmith, W. and Sackman, J. L., (1979).Longitudinal Waves in Liquid-Filled Tubes—II: Experiments,*International Journal of Mechanical Sciences*, Vol. 21, pp. 223–236.

Conceicao, S.I., Olhero, S., Velho, J.L., Ferreira, J.M.F.,(2003).Influence of Shear Intensity During Slip Preparation on Rheological Characteristics of Calcium Carbonate Suspensions, *Ceramics International*, Vol.29, pp.365–370.

Han, W., Dong, Z. and Chai, H., (1998).Water Hammer in Pipeline with Hyperconcentrated Slurry Flows Carrying Solid Particles, *Science in China (Series E)*, Vol. 41.

Inaba, K., Takahashi, H., Kollika, N. and Kishimoto K., (2010).Visualization and Measurement of Wave Propagations in Slurry Hammers, *Proceedings of the SEM2010,* pp.1–7.

Joukowsky, N., (1900).Über den HydraulischenStoss in Wasserleitungsrohren, *Mémoire de l'AcademieImpériale des Sciences*, *St. Petersburg*, 8th Series, Vol. IX.

Kuhl, E., Hulshoff, S. and Borst, R. de, (2003).An Arbitrary LagrangianEulerian Finite–Element Approach for Fluid–Structure Interaction Phenomena, *International Journal for Numerical Methods in Engineering*, Vol.57, pp.117–142.

Kugge, C. and Daicic, J., (2004).Shear Response of Concentrated Calcium Carbonate Suspensions, *Journal of Colloid and Interface Science*, Vol.271, pp.241–248.

Livermore Software Technology Corporation, (2007). *LS-DYNA Keyword User's Manual Version 971*.

Meyers, M. A., ,(1994). Dynamic Behavior of materials,*Wiley-Interscience*,*New York.*

Russel, W.B., Saville, D.A., (1989). Schowalter, W.R., Colloidal Dispersions, *Cambridge University Press*.

Shepherd, J. E., (2009).Structural Response of Piping to Internal Gas Detonation, *Journal of Pressure Vessel Technology*, Vol.131, 031204 (pp.1–13).

Skalak, R., (1955/1956).An Extension of the Theory of Water Hammer, *Water Power*,Vol. 7/8, pp. 458–462/17–22.

Skalak, R., (1956).An Extension of the Theory of Water Hammer, *Transaction of the ASME*, Vol. 78, pp. 105–116.

Souli, M., Ouahsine, A. and Lewin, L., (2000). ALE Formulation for Fluid-Structure Interaction Problems, *Computational Methods in Applied Mechanics and Engineering*, Vol.190, pp.659–675.

Tijsseling, A.S, (1993).Fluid-Structure Interaction in Case of Water Hammer with Cavitation, *Doctoral Thesis*.

Tijsseling, A. S., Lambert, M. F., Simpson, A. R., Stephens, M.L., Vítkovský, J. P. andBergant, A., Skalak's Extended Theory of Water Hammer, *Journal of Sounds and Vibration*, Vol. 310, pp. 718–728, (2008).

Tijsseling, A.S, (2007). Water Hammer with Fluid-structure Interaction in Thick-Walled Pipes, *Journal of Computers and Structures*, Vol.85, pp.844–851.